

# Field-Effect Transistors Based on Langmuir–Blodgett Films of Phthalocyanine Derivatives as Semiconductor Layers

Kai Xiao, Yunqi Liu,\* Xuebin Huang, Yu Xu, Gui Yu, and Daoben Zhu\*

Center for Molecular Science, Institute of Chemistry, Chinese Academy of Sciences,  
Beijing 100080, People's Republic of China

Received: April 8, 2003; In Final Form: June 23, 2003

Two soluble phthalocyanine derivatives, 2,9,16-tri(*tert*-butyl)-23-(10-hydroxydecyloxy) phthalocyanine (**1**) and 2,9,16-tri(*tert*-butyl)-23-(10-hydroxydecyloxy) copper phthalocyanine (**2**) were used as semiconductor layers in organic thin-film transistors (OTFTs) based on their Langmuir–Blodgett (LB) films. From the  $\pi$ – $A$  curves, we can conclude that the phthalocyanine **1** and **2** molecules are in a tilted arrangement at the air–water interface. The molecular ordering in the LB multilayer films on the SiO<sub>2</sub> substrate was examined by using UV–Vis absorption spectra and atomic force microscopy (AFM). The highest occupied molecular orbital and the lowest unoccupied molecular orbital were determined, and the energy band diagram of their OTFTs can be deduced by the cyclic voltammetric measurements. The LB films of phthalocyanine **1** and **2** were subsequently made into p-channel field-effect transistors, which were generally operated in the enhanced mode. The channel mobilities of phthalocyanine **1** and **2** were calculated to be about  $4.8 \times 10^{-5} \text{ cm}^2 \text{ V}^{-1} \text{ s}^{-1}$  and  $4.0 \times 10^{-4} \text{ cm}^2 \text{ V}^{-1} \text{ s}^{-1}$ , respectively.

## Introduction

Recently, electrically active organic compounds as semiconducting materials in thin-film transistors (TFTs) are of great interest for several low-cost or large-area electronics applications in polymeric substrate like flat-panel displays, smart cards, and radio frequency identification tags.<sup>1–5</sup> Phthalocyanine (Pc) derivatives have been used for TFTs as very promising active organic semiconducting materials. The family of Pc exhibits remarkable chemical and thermal stabilities to various environments in comparison with those of other organic semiconductors.<sup>6</sup> As the most investigated member of the Pc series, CuPc and CuPc-F have been utilized for their potential application in organic thin film transistors.<sup>7,8</sup> Strong intermolecular interactions existing in the solid state of Pc are believed to originate from the strong  $\pi$ – $\pi$  interactions resulting in decreased solubility with common solvents. As a result, most of the devices based on Pc have to be fabricated by vacuum sublimation. However, the most attractive thin film deposition (spin coating, molecular assemblies, Langmuir–Blodgett (LB), etc.) and patterning (nonlithographic and lithographic) methods are likely to be solution-based. If organic semiconductors are going to compete with their inorganic counterpart, low-cost techniques such as solution deposition or printing techniques offer the greatest advantages. Thus, to increase solution processability, substitution has been introduced to the molecule. Modifying the macro ring with substituent groups at their peripheral ring can enhance the solubility of Pc's.<sup>9,10</sup> As reported recently,<sup>11</sup> we have succeeded in preparing two new Pc derivatives named 2,9,16-tri(*tert*-butyl)-23-(10-hydroxydecyloxy) phthalocyanine (**1**) and 2,9,16-tri(*tert*-butyl)-23-(10-hydroxydecyloxy) copper phthalocyanine (**2**). These materials all exhibited good solubility in common organic solvents such as chloroform, acetonitrile, and toluene. It is well-

known that the LB technique enables one to gain direct access to precise thickness and orientation controls on the molecular level, and thus this method seems to be most effective for realizing well-defined Pc thin films for constructing thin film transistors.<sup>12–15</sup> The first LB–FET used regiorandom poly(3-alkylthiophene)s (PAT) as the semiconducting material. The random position of the side chains in the regiorandom poly(3-alkylthiophene) (RI–PAT) inhibits the  $\pi$ – $\pi$  stacking and reduces the crystallinity of the film. Consequently, the field-effect mobility in the RI–PAT FET is low,  $10^{-7}$ – $10^{-4} \text{ cm}^2 \text{ V}^{-1} \text{ s}^{-1}$ .<sup>16</sup> Regioregular poly(3-alkylthiophene) (RR–P3HT) is likely to form stable Langmuir films due to its hairy-rodlike polymer structure.<sup>13</sup> Hu and co-workers have reported the OFET using amino-tri-*tert*-butyl-phthalocyanine LB films as the semiconductor layers, and the mobility was about  $5.2 \times 10^{-6} \text{ cm}^2 \text{ V}^{-1} \text{ s}^{-1}$ .<sup>14</sup> Locklin and co-workers fabricated the OTFT of water-soluble cationic and anionic phthalocyanine derivatives using the layer-by-layer deposition technique, and the field-effect mobility could reach  $1.46 \times 10^{-5}$  to  $9.09 \times 10^{-4} \text{ cm}^2 \text{ V}^{-1} \text{ s}^{-1}$ .<sup>17</sup>

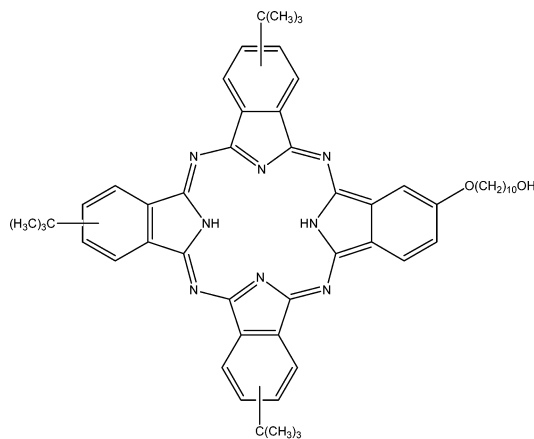
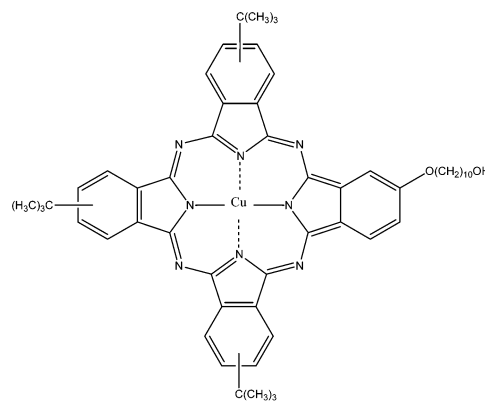
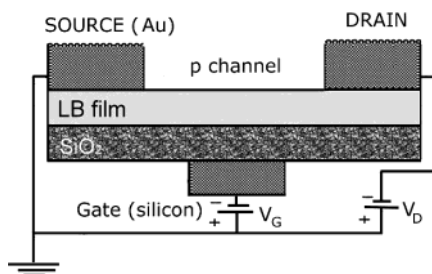
In this paper, we fabricate organic thin-film transistors by applying the LB technique to phthalocyanine **1** and **2** and study the characterization of their physical properties, such as surface pressure–area isotherms, spectroscopic and electrochemical characteristics, and field-effect mobilities.

## Experimental Section

**Materials and LB Film Fabrication.** The chemical structure of Pc molecules used in our experiments is shown in Figure 1, and phthalocyanines **1** and **2** were synthesized following the procedure described previously.<sup>11</sup> Surface pressure–area isotherm measurements and deposition experiments were performed on a fully automatic KSV-5000 instrument (Finland). Phthalocyanines **1** or **2** dissolved in chloroform (0.6 mM) were spread onto double-distilled water. At a constant pressure of 22 mN/m, the floating layers on the subphase were transferred

\* Corresponding authors. Tel: +86-10-6261-3253. Fax: +86-10-6255-9373.

E-mail: liuyq@iccas.ac.cn.

**1****2****Figure 1.** Chemical structures of phthalocyanine **1** and **2** molecules.**Figure 2.** Schematic view of OTFTs based on the LB films of phthalocyanine **1** and **2**.

to SiO<sub>2</sub>/Si substrates by the vertical dipping method in a speed range of 1 mm/min.

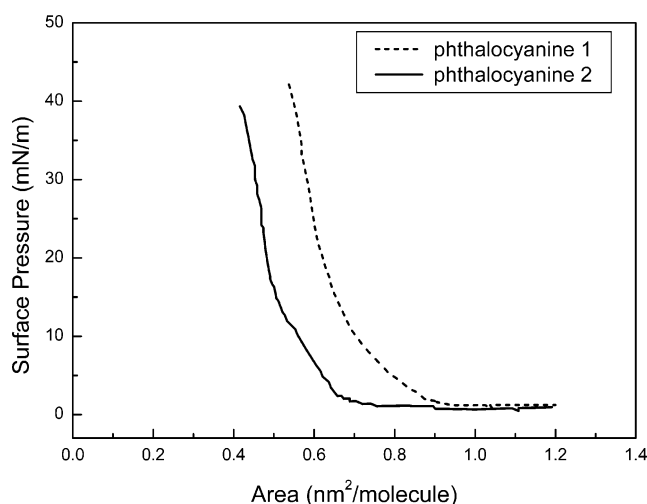
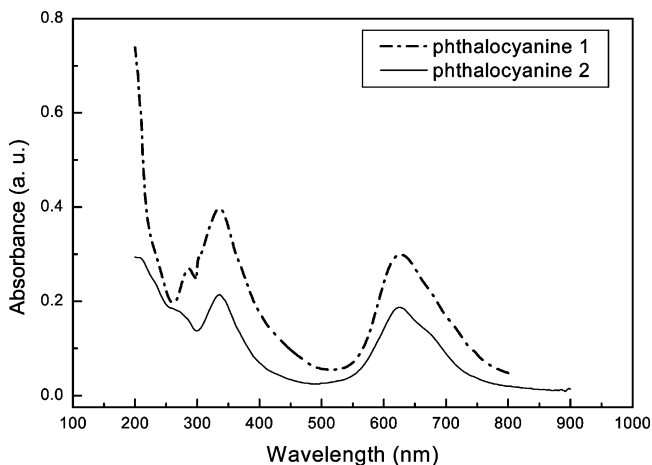
**Thin Film Characterization.** The UV–Vis spectra of the LB films on the quartz were recorded on a Shimadzu UV-3100 spectrometer using blank quartz as reference. The topography and morphology of the phthalocyanine **1** and **2** LB films on Si/SiO<sub>2</sub> were studied in air using a Digital Instruments nanoprobe atomic force microscopic (AFM) in contacting mode with a 10  $\mu$ m scanner.

**Electrochemical Characterization.** Cyclic voltammetric measurements were recorded on a computer-controlled EG&G Potentiostat/Galvanostat model 283 at room temperature. A platinum/carbon plate was used as the working electrode, a platinum wire as the counter electrode, and Ag/Ag<sup>+</sup> as the reference electrode, respectively. Tetrahydrofuran was used as the solvent for phthalocyanine **1** and **2**. The measurement was performed in solution containing  $1 \times 10^{-4}$  mol/L Pc's. Before measurements, the solution was deoxygenated by argon bubbling for about five minutes.

**FET Structure and Characterization.** The transistor device structure is shown in Figure 2. The n-doped Si substrate functions as the gate, and an oxide layer of 400 nm is the gate dielectric having a capacitance per unit area of 10 nF/cm<sup>2</sup>. The drain and source electrodes were vacuum deposited using a shadow mask. These electrode have widths  $W = 34$  mm and channel length  $L = 200$   $\mu$ m. The electric characteristics of these devices were measured under air. The current–voltage characteristics were obtained with a Hewlett-Packard (HP) 4140B parameter analyzer at room temperature.

## Results and Discussion

**Formation of LB Films.** The surface pressure–area isotherms of phthalocyanine **1** and **2** are shown in Figure 3. The

**Figure 3.** Surface pressure–area isotherms of phthalocyanine **1** and **2** at room temperature.**Figure 4.** UV–Vis absorption spectra of 12-layer phthalocyanine **1** and **2** LB films.

steeply inclining part corresponding to formation of the solid monolayer and the high surface pressure of the collapse point of the monolayer indicate the good film-forming behavior of the phthalocyanine compounds. From the surface pressure–area isotherms, the limiting area per molecule of phthalocyanine **1** and **2** was estimated to be 71.0 and 58.7  $\text{\AA}^2$ , respectively. These values are useful for estimating the configuration of phthalocyanine molecules at the air–water interface. The diagonal

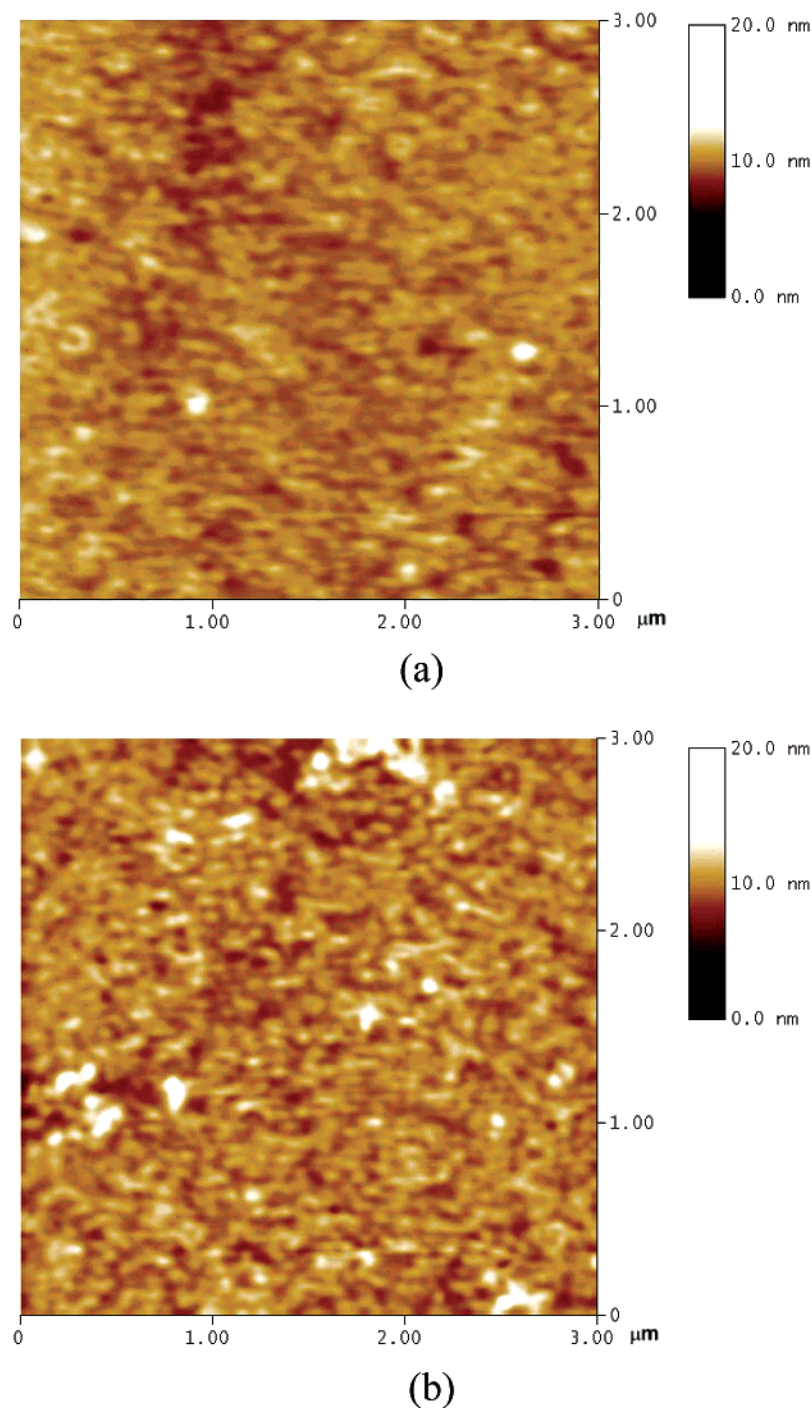


**Figure 5.**  $3\ \mu\text{m} \times 3\ \mu\text{m}$  atomic force microscope (AFM) images of 12-layer phthalocyanine **1** (a) and **2** (b) films transferred onto the  $\text{SiO}_2$  surface at room temperature.

distance across a molecule of *tert*-butyl-substituted phthalocyanine is approximately  $19.5\ \text{\AA}$ , as calculated by Hua et al.<sup>18</sup> In our case, the phthalocyanine is substituted with three *tert*-butyl groups and one hydroxydecyloxy group. Therefore, a planar view of the molecule is as a square with a side length of  $13.8\ \text{\AA}$  ( $19.5 \times 2^{-0.5}$ ), even though one diagonal distance is greater than  $19.5\ \text{\AA}$ . If the molecules of phthalocyanine **1** and **2** are densely stacked in a face-to-face orientation and edge-on to the water surface, the average area per molecule would be approximately  $46.9\ \text{\AA}^2$  ( $13.8\ \text{\AA} \times 3.4\ \text{\AA}$ ), assuming that the “thickness” of the Pc is  $3.4\ \text{\AA}$ . However, if the molecules of Pc’s are laid down flat on the water surface, the average area per molecule would be approximately  $190.4\ \text{\AA}^2$  ( $13.8\ \text{\AA} \times 13.8\ \text{\AA}$ ). Since the limiting area per molecule from the isotherm is

between the two calculated values mentioned above, it is reasonable to consider that phthalocyanine **1** and **2** molecules are in a tilted arrangement to the water surface, and the tilt angles were about  $68^\circ$  and  $72^\circ$ , respectively. We can also conclude the face-to-face stacking of the phthalocyanine **2** molecules arranged more closely due to the larger tilt angles than that of phthalocyanine **1** molecules.

**Optical Absorption.** Figure 4 shows the UV–Vis spectra of the 12-layer phthalocyanine **1** and **2** LB films. The spectra in the Q-band region exhibited intense absorption around  $620\ \text{nm}$  due to aggregated species, which were attributed to the development of a face-to-face stacking of the Pc molecules.<sup>19</sup> Also, weak shoulders were observed at the lower energy side of the UV–Vis spectra of the phthalocyanine **2** assigned to the

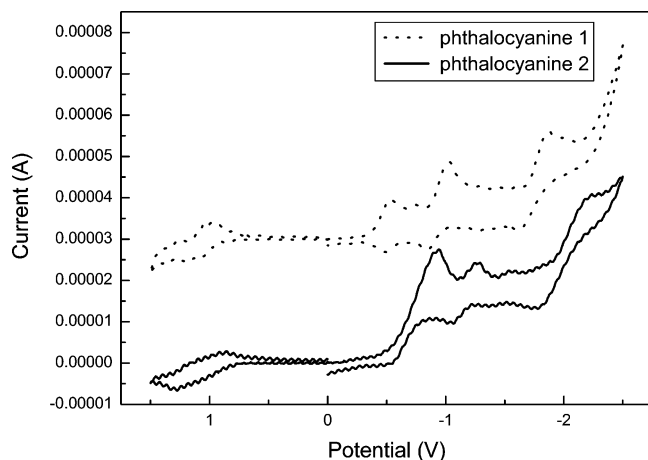


**Figure 6.** Cyclic voltammograms of phthalocyanine **1** and phthalocyanine **2** in a tetrahydrofuran solution at a scan rate of 40 mV s<sup>-1</sup>.

monomeric ones. The average orientation of the Pc stacking has been examined by using polarized electronic adsorption spectroscopy, and it was reported that the Pc molecules stood obliquely with an edge-on configuration on the substrate surface which was favorable for the operation of a FET.<sup>20</sup> The band edge has been assigned to a  $\pi$ - $\pi^*$  transition from the highest occupied molecular orbital (HOMO) to the lowest unoccupied molecular orbital (LUMO) through extended Huckel calculations.<sup>21</sup> By extrapolating the absorption spectrum at the long-wavelength side, the optical band gaps are estimated to be in the range of 1.1–1.3 eV.

**AFM Measurements.** The LB films were also characterized by the investigation of AFM (Figure 5). The images of the 12-layer phthalocyanine **1** and **2** LB films transferred directly onto the SiO<sub>2</sub> surface were observed over the area of 3  $\mu$ m  $\times$  3  $\mu$ m in a contact mode. Their figures show that the phthalocyanine **1** and **2** molecules are homogeneously arranged. The average large grain size of phthalocyanine **1** and **2** films are about 30–50 nm.

**Energy Level.** Let us now consider the relevant energy levels in the materials considered in OTFT, and how these could affect transport properties. The energy levels of the highest unoccupied LUMO and HOMO can be obtained by the cyclic voltammetric measurement. Cyclic voltammogram (CV) of phthalocyanine **1** and **2** over the range of +1.5 to -2.0 V exhibited four couple peaks of oxidation and reduction, respectively (Figure 6). The potential of the first ring reduction and the first ring oxidation is related to an energy level of its LUMO and HOMO.<sup>22,23</sup> Thus, from the data of CV, the LUMO and HOMO of phthalocyanine **1** and **2** can be approximated about -4.29 eV, -5.44 eV and -4.12 eV, -5.35 eV, respectively. The similar HOMO-LUMO gaps of phthalocyanine **1** and **2** indicate that they possess narrower energy gaps than that of other symmetrical Pc's due to the donor substituted group. Therefore, the electron-acceptor (D-A) abilities of Pc's will be greatly improved for the linked donors pushing the electron to the macro ring of Pc's. The narrower energy gap of phthalocyanine **1** and **2** is easier for electron or holes entering the channel as needed, without creating chemical instability. Too high a band gap would probably mean that the bands themselves would be too far in energy from the voltage-modified charge carrier energies at the semiconductor interface.<sup>24</sup>

Organic TFTs based on the LB films of phthalocyanine **1** and **2** are generally operated in the enhanced mode, and in Figure 7 the sketch of the energy band diagram gives evidence of the formation of a two-dimensional accumulation layer for

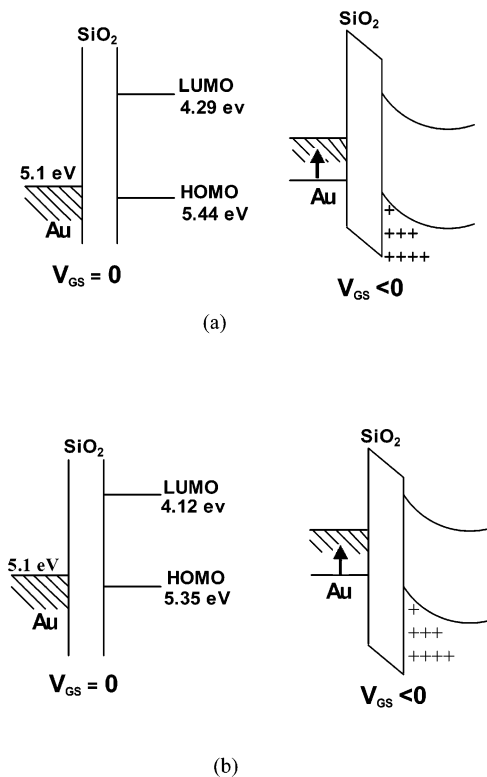


**Figure 7.** Schematic energy-band diagram for phthalocyanine **1** (a) and **2** (b) TFTs, the left side shows the devices at no gate bias. Whereas, on the right side, the p-channel devices is negatively biased. The highest occupied molecular orbital (HOMO) and the lowest unoccupied molecular orbital (LUMO) are shown for both materials as well.

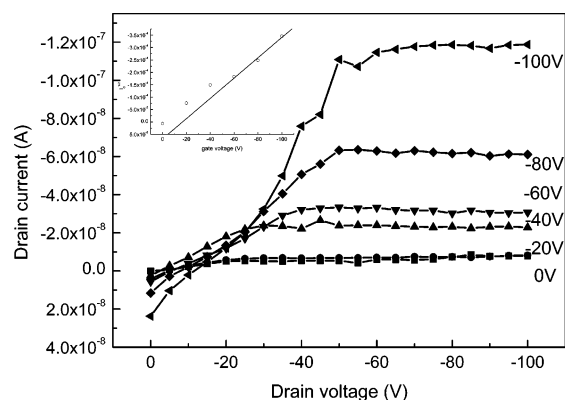
p-channel devices. It is quite evident from the data depicted in Figure 7 that the energy barrier exist between the Au source/drain (S/D) electrodes and the LUMO/HOMO of Pc. This does not present a serious problem because the FET channel becomes highly conducting in the on state due to the large induced charge density. Thus, the energy barrier between the Au contacts and the Pc HOMO is unlikely to be the cause of the absence of observable hole transport parallel to the molecular planes.<sup>25</sup>

**FET Characterization.** The LB films were subsequently made into field-effect transistor devices to test their charge-carrier mobility. The cross-sectional view of the transistor device structure is shown in Figure 2, and its preparation has been previously described.<sup>15</sup> Figure 8 shows typical  $I$ - $V$  curves acquired from devices operating in the accumulation mode. The drain-source currents of negative sign scale-up with negative gate voltage. At the saturated region,  $I_{DS}$  can be described using eq 1:<sup>26</sup>

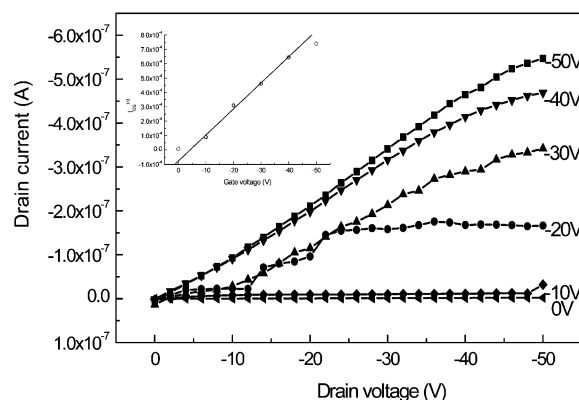
$$I_{DS} = \frac{WC_i}{2L} \mu (V_G - V_0)^2 \quad (1)$$

where  $\mu$  is the field-effect mobility,  $W$  is the channel width,  $L$  is the channel length, and  $C_i$  is the capacitance per unit area of the insulating layer (SiO<sub>2</sub>, 400 nm,  $C_i$ , 10 nF/cm<sup>2</sup>). A plot of  $I_{DS}^{1/2}$  vs  $V_G$  can be used to obtain  $V_0$ , the extrapolation to the  $V_G$  axis. The field-effect mobility can then be calculated from eq 1. The field-effect mobilities measured in the saturation regime were about  $4.8 \times 10^{-5}$  and  $4.0 \times 10^{-4}$  cm<sup>2</sup> V<sup>-1</sup> s<sup>-1</sup> for phthalocyanine **1** and **2** 12-layer LB TFTs, respectively. The mobility of the phthalocyanine **2** is relatively 10 times larger than that of phthalocyanine **1**. The more closely face-to-face stacking of phthalocyanine **2** molecule makes it easy for the carriers transporting in the LB films. The mobility of the devices





(a)



(b)

**Figure 8.** Drain current and drain voltage characteristics of transistors prepared from 12-layer phthalocyanine **1** (a) and **2** (b) LB films. The inset shows the plot of the square root of drain current versus gate voltage, used to calculate threshold voltage and mobility.

was insensitive to the thickness of the films. Devices composed of 10 to 20 layers had very similar mobilities. Therefore, the charge carriers were assumed to be confined within the first few molecular layers of the films.<sup>13</sup> With our TFTs using substituted phthalocyanine-active LB films, the device performance is lower than that of RR-P3AT LB TFTs. Because RR-P3AT has hairy-rodlike polymer structure laying flat on the surface. The rodlike segments are ordered in a parallel lamellatype stack with interdigitated alkyl side chains to achieve maximum van der Waals interactions. The transferred LB films were oriented with the polymer backbone parallel to the substrate in an edge-on conformation, which is favorable for the operation of a FET. Our Pc derivatives as small molecules have good solubility in common organic solvents through chemical structure modification, but this perhaps affects the planarity of the  $\pi$ -system and more importantly its ability to pack in a structure where charge carriers cannot move freely. Therefore, to improve the carrier mobility of Pc films, the molecules of Pc compounds should be assembled in a face-to-face arrangement through a more highly ordered film with improved interchain distance and  $\pi$ - $\pi$  interaction and decrease the pinholes and defects to result in a better quality and continuity of the LB films throughout the FET channel. Nevertheless, the results of using Pc derivative LB film are promising and competitive with that of vacuum deposition as small molecules.

## Conclusions

We investigated the characteristics of Langmuir-Blodgett films of phthalocyanine **1** and **2**. In all the cases, the phthalocyanine **1** and **2** molecules were found to be stacked face-to-face with a tilt angle configuration on the substrate surface. Their narrower energy gaps are easier for electron or holes entering the channel as needed. Therefore, the OTFT based on phthalocyanine **1** and **2** LB films were successfully prepared and showed p-channel accumulation devices. From the electrical properties of the OTFTs, the mobilities of phthalocyanine **1** and **2** were calculated to be about  $4.8 \times 10^{-5}$  and  $4.0 \times 10^{-4}$   $\text{cm}^2 \text{V}^{-1} \text{s}^{-1}$ , respectively.

**Acknowledgment.** Financial support from the National Natural Science Foundation, the Major State Basic Research Development Program and the Chinese Academy of Sciences is gratefully acknowledged.

## References and Notes

- (1) Drury, C.; Mutsaers, C.; Hart, C.; Matters, M.; de Leeuw, D. *Appl. Phys. Lett.* **1998**, *73*, 108.
- (2) Gelinck, G. H.; Geuns, T. C. T.; de Leeuw, D. *Appl. Phys. Lett.* **2000**, *77*, 1487.
- (3) Sheraw, C. D.; Zhou, L.; Huang, J. R.; Gundlach, D. J.; Jackson, T. N.; Kane, M. G.; Hill, I. G.; Hammond, M. S.; Campi, J.; Greening, B. K.; Franci, J.; West J. *Appl. Phys. Lett.* **2002**, *80*, 1088.
- (4) Huitema, H. E. A.; Gelinck, G. H.; van der Putten, J. B. P. H.; Kuijk, K. E.; Hart, C.; Cantatore, E.; Herwig, P. T.; van Breemen, A. J. J. M.; Leeuw, D. M. *Nature* **2001**, *414*, 599.
- (5) Mach, P.; Rodriguez, S. J.; Nortrup, R.; Wiltzius, P.; Rogers, J. A. *Appl. Phys. Lett.* **2001**, *78*, 3592.
- (6) Snow, A. W.; Barger, W. R. Phthalocyanine Films in Chemical Sensors. In *Phthalocyanines—Properties and Applications*, Vol. 1; Lezonff, C. C.; Lever, A. B. P., Eds.; VCH: New York, 1989.
- (7) Bao, Z. N.; Lovinger, A. J.; Dodabalapur, A. *Appl. Phys. Lett.* **1996**, *69*, 3066.
- (8) Bao, Z. N.; Lovinger, A. J.; Dodabalapur, A. *Adv. Mater.* **1997**, *9*, 42.
- (9) Liu, Y. Q.; Xu, Y.; Zhu, D. B.; Wada, T.; Sasabe, H.; Zhao, X. S.; Xie, X. M. *J. Phys. Chem.* **1995**, *9*, 6958.
- (10) Liu, S. G.; Liu, Y. Q.; Xu, Y.; Zhu, D. B.; Yu, A. C.; Zhao, X. S. *Langmuir* **1998**, *14*, 690.
- (11) Huang, X. B.; Liu, Y. Q.; Wang, S.; Zhou, S. Q.; Zhu, D. B. *Chem. Eur. J.* **2002**, *8*, 4179.
- (12) Paloheimo, J.; Stubb, H.; Yli-Lahti, P.; Dyreklev, P.; Inganas, O. *Thin Solid Films* **1992**, *210–211*, 283.
- (13) Xu, G. F.; Bao, Z. N.; Groves, J. T. *Langmuir* **2000**, *16*, 1834.
- (14) Hu, W. P.; Liu, Y. Q.; Liu, S. G.; Zhou, S. Q.; Zhu, D. B. *Synth. Met.* **1999**, *104*, 19.
- (15) Liu, Y. Q.; Hu, W. P.; Qiu, W. F.; Xu, Y.; Zhou, S. Q.; Zhu, D. B. *Sens. Actuators, B* **2001**, *80*, 202.
- (16) Paloheimo, J.; Kuivalainen, P.; Stubb, H.; Vuorimaa, E.; Yli-Lahti, P. *Appl. Phys. Lett.* **1990**, *56*, 1157.
- (17) Lochlin, J.; Shinbo, K.; Onishi, K.; Kaneko, F.; Bao, Z. N.; Advincula, R. C. *Chem. Mater.* **2003**, *15*, 1404.
- (18) Hua, Y. L.; Roberts, G.; Ahmad, M. M.; Petty, M. C. *Philos. Mag. B* **1986**, *53*, 105.
- (19) Xiang, H. Q.; Tanaka, K.; Kajiyama, T. *Langmuir* **2002**, *18*, 9102.
- (20) Xiang, H. Q.; Tanaka, K.; Takahara, A.; Kajiyama, T. *Langmuir* **2002**, *18*, 2223.
- (21) Schaffwe, A. M.; Gouterman, M.; Davidson, E. *Theor. Chim. Acta* **1973**, *30*, 9.
- (22) Boronat, M.; Viruela, R.; Ort, E. *Synth. Met.* **1995**, *71*, 2291.
- (23) Lever, A. B. P.; Minor, P. C. *Inorg. Chem.* **1981**, *20*, 4015.
- (24) Katz, H. E.; Bao, Z. *J. Phys. Chem. B* **2000**, *104*, 671.
- (25) Ostrick, J. R.; Dodabalapur, A.; Torsi, L.; Lovinger, A. J.; Kwock, E. W.; Miller, T. M.; Galvin, M.; Berggren, M.; Katz, H. E. *J. Appl. Phys.* **1997**, *81*, 6804.
- (26) Sze, S. M.; *Physics of Semiconductor Devices*; John Wiley & Sons: New York, 1981.